DOI: 10.1002/chem.201203455

Parahydrogen-Induced Polarization Transfer to ^{19}F in Perfluorocarbons for ^{19}F NMR Spectroscopy and MRI**

Markus Plaumann,*[a] Ute Bommerich,[b] Thomas Trantzschel,[a] Denise Lego,[b] Sonja Dillenberger,[c] Grit Sauer,[c] Joachim Bargon,[d] Gerd Buntkowsky,[c] and Johannes Bernarding[a]

Abstract: Fluorinated substances are important in chemistry, industry, and the life sciences. In a new approach, parahydrogen-induced polarization (PHIP) is applied to enhance ^{19}F MR signals of (perfluoro-*n*-hexyl)ethene and (perfluoro-*n*-hexyl)ethane. Unexpectedly, the end-standing CF_3 group exhibits the highest amount of polarization despite the negligible coupling to the added protons. To clarify this non-intuitive distribution of polarization, signal enhancements in deuterated chloroform and acetone were compared and ^{19}F–^{19}F NOESY spectra, as well as ^{19}F T_1 values were measured by NMR spectroscopy. By using the well separated and enhanced signal of the CF_3 group, first ^{19}F MR images of hyperpolarized linear semifluorinated alkenes were recorded.

Keywords: fluorine · hydrogenation · imaging agents · NMR spectroscopy · polarization transfer

Introduction

In the last few years, perfluorinated molecules have been raising increasing interest. They are of great relevance in technical, chemical, and life science applications due to their manifold, excellent characteristics.[1] One of the most studied perfluorinated compounds in medicine is the linear perfluorooctylbromide ($C_8F_{15}Br$), also known as perflubron, which can be used as a blood substitute as well as a contrast agent in ^{19}F magnetic resonance imaging (MRI).[2] In general, perfluorocarbons are well known from in vivo studies in different applications, for example, artificial blood, liquid breathing,[3] and in ^{19}F MRI studies.[4]

^{19}F NMR spectroscopy has a long-standing history in high-resolution NMR spectroscopy as there is a high chemical-shift range of more than 300 ppm and no natural fluorine background signal in biological organisms. Therefore, signals can be attributed unambiguously. Similarly, ^{19}F MRI has recently become an important research topic in medicine with a focus on molecular imaging applications, lung imaging, and drug monitoring.[5] Although this shows that ^{19}F MRI has a high potential to serve as a new diagnostic tool, the in vivo spin density of most substrates is rather small, leading to low signal-to-noise ratios (SNRs). Hence, strong efforts aim to increase the ^{19}F SNR as the prerequisite to establish MR in clinical and medical routine.

Instead of increasing the external polarizing magnetic field, less costly but very efficient non-standard polarization methods offer a new way to acquire signals with higher SNR. Hyperpolarization techniques such as dynamic nuclear polarization (DNP), chemically induced dynamic nuclear polarization (CIDNP), spin-exchange optical pumping (SEOP), and parahydrogen-induced polarization (PHIP) can be used to enhance the SNR in MR experiments up to several orders of magnitude. In general, these methods generate populations of the Zeeman energy levels that differ significantly from the limited thermal polarization.[6,7] PHIP is advantageous because its implementation requires less technological effort. PHIP signals depend on whether hydrogenation is performed in the presence of a strong magnetic field (PASADENA, parahydrogen and synthesis allow dramatically enhanced nuclear alignment),[8] or whether hydrogenation occurs under low-field conditions (ALTADENA, adiabatic longitudinal transfer after dissociation engenders net alignment) followed by adiabatic transport into the detection field.[9]

PHIP can be used, for example, for analyzing intermediates and products of catalytic reactions or, as recently reported, also for biological and medical studies by polariza-

[a] Dr. M. Plaumann, Dipl.-Phys. T. Trantzschel, Prof. Dr. J. Bernarding
Department of Biometry and Medical Informatics
Otto-von-Guericke University of Magdeburg
Leipziger Strasse 44, 39120 Magdeburg (Germany)
Fax: (+49) 391-67-13536
E-mail: markus.plaumann@med.ovgu.de

[b] Dr. U. Bommerich, Dipl.-Ing. D. Lego
Leibniz-Institute for Neurobiology
39118 Magdeburg (Germany)

[c] Dipl.-Chem. S. Dillenberger, Dipl.-Chem. G. Sauer,
Prof. Dr. G. Buntkowsky
Eduard-Zintl-Institute for Inorganic Chemistry
Technical University Darmstadt
64287 Darmstadt (Germany)

[d] Prof. Dr. J. Bargon
Institute of Physical and Theoretical Chemistry
University Bonn, 53115 Bonn (Germany)

[**] MRI = magnetic resonance imaging.

Supporting information for this article is available on the WWW under http://dx.doi.org/10.1002/chem.201203455.

tion transfer to heteronuclei, mostly ^{13}C.[10] The transfer of proton hyperpolarization to heteronuclei such as ^{13}C, ^{15}N, ^{31}P, or ^{19}F through scalar couplings has been successfully demonstrated. This enables the development of contrast agents for MRI by using PHIP to hyperpolarize ^{13}C or ^{19}F in these substrates.[7,11,12]

However, the transfer of PHIP to ^{19}F is documented only for a small class of closely related aromatic systems, which are potentially harmful.[12,13]

In order to extend this method to biocompatible substrates, we attempted to hyperpolarize the linear (perfluoro-*n*-hexyl)ethene (PFE2) and (perfluoro-*n*-hexyl)ethane (PFE1) through PHIP (Scheme 1). Both molecules have the

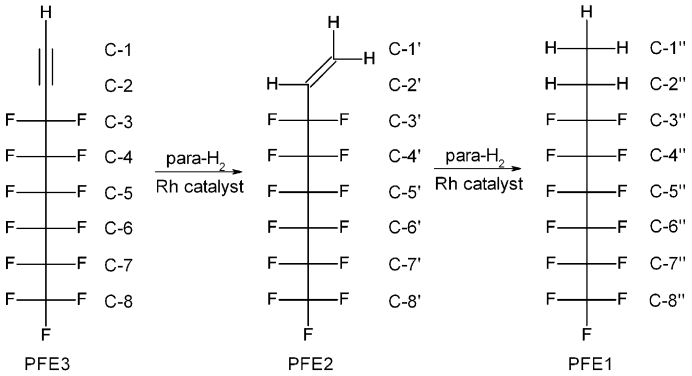

Scheme 1. Reaction scheme of the hydrogenation of PFE3 to PFE2 and the further hydrogenation to PFE1.

same number of carbon atoms as the perfluorooctylbromide previously mentioned; therefore, they should be applicable for in vivo studies. The hyperpolarization of PFE1 is particularly interesting because semifluorinated alkanes are physiologically inert.[14] In addition, they might be used for in vivo monitoring of inflammatory processes.[15]

Results and Discussion

At first, feasibility experiments for hydrogenation of (perfluoro-*n*-hexyl)ethyne (PFE3) in [D_6]acetone were performed in the presence of [Rh(cod)(dppb)]BF_4 (cod = 1,5-cyclooctadiene, dppb = 1,4-bis(diphenylphosphino)butane) as a catalytic system. The ^1H NMR spectra show antiphase signals with signal-enhancement (SE) factors of 111 for the CH group (C-2′) at $\delta = 6.26$ ppm and 139 for the added proton on the CH_2 group (C-1′) of PFE2 at $\delta = 6.04$ ppm (Figure 1).

Additionally, hydrogenation from PFE2 to the saturated PFE1 was measured. The corresponding ^1H NMR spectrum (Figure 2) shows signals with an SE of two for the newly formed CH_3 (C-1″) at $\delta = 1.17$ ppm and 1.5 for the CH_2 group (C-2″) at $\delta = 2.27$ ppm. These smaller SE factors might be caused by a small conversion rate of the double-bond system.[16]

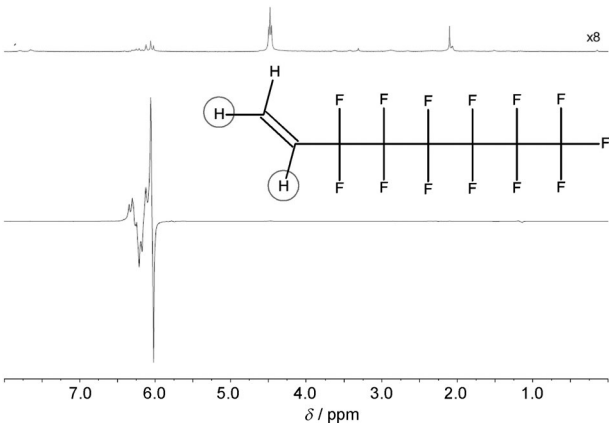

Figure 1. ^1H NMR spectra measured in [D_6]acetone. Hyperpolarized (perfluoro-*n*-hexyl)ethene (bottom) and its spectrum in thermal equilibrium in eightfold magnification (top). Cycles indicate the transferred protons.

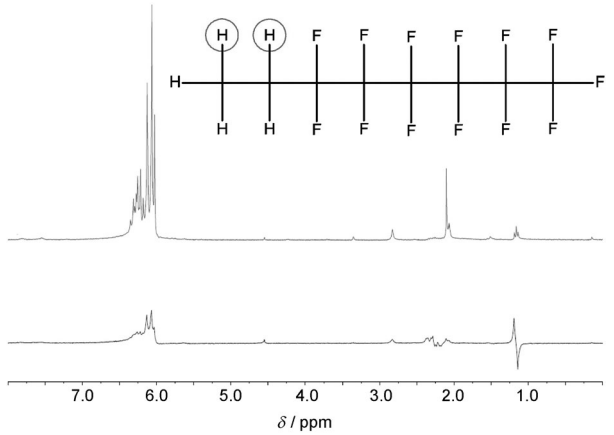

Figure 2. ^1H NMR spectra measured in [D_6]acetone. Hyperpolarized (perfluoro-*n*-hexyl)ethane (bottom) and its spectrum in thermal equilibrium (top). Cycles indicate the transferred protons.

After the successful hydrogenation and ^1H hyperpolarization of these model compounds, the polarization transfer to fluorine was examined.

For the interpretation of the ^{19}F PHIP NMR and MRI data a correct signal assignment of the different fluorine groups is essential. It is well known that $^4J(F,F)$ couplings in perfluoroalkyl chains are generally larger than $^3J(F,F)$ or $^5J(F,F)$ values.[17] These correlations, observable in ^{19}F–^{19}F COSY spectra, were used to assign the signals (see the Supporting Information). Figure 3 shows the ^{19}F NMR spectra of the three molecules discussed here with the corresponding notations.

From comparison with proton-decoupled ^{19}F NMR spectra of PFE2 and PFE1 it can be concluded that only fluorine atoms bound to C-3′, respectively C-3″, exhibit a coupling to the protons (Figures S7 and S8 in the Supporting Information).

The ^{19}F PHIP NMR spectrum measured directly after hydrogenation of PFE3 is shown in Figure 4. Except for C-5′ ($\delta = -122.4$ ppm) and C-6′ ($\delta = -123.7$ ppm), all other moi-

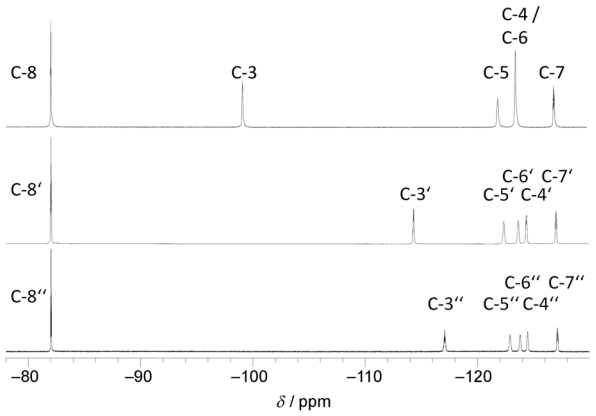

Figure 3. ^{19}F NMR spectra and the corresponding signal assignments of (perfluoro-*n*-hexyl)ethyne (PFE3; top), (perfluoro-*n*-hexyl)ethene (PFE2; middel), and (perfluoro-*n*-hexyl)ethane (PFE1; bottom) measured in [D_6]acetone.

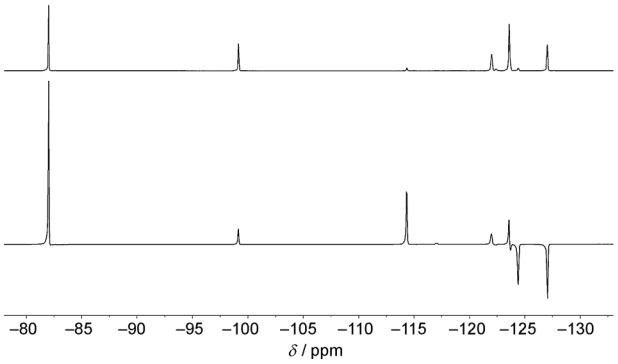

Figure 4. ^{19}F NMR spectrum taken directly after hydrogenation of PFE3 showing signals of hyperpolarized PFE2 (bottom) and the corresponding spectrum detected at thermal equilibrium (top).

eties exhibit notable SE factors. Signals of fluorine bound to C-3′ ($\delta = -114.4$ ppm, SE = 11) and C-8′ ($\delta = -82.0$ ppm, SE = 15) show in-phase patterns, whereas emission phase signals can be observed for fluorine bound to C-4′ ($\delta = -124.4$ ppm, SE = 26) and C-7′ ($\delta = -127.1$ ppm, SE = 3).

For sake of clarity the calculation of the SE factors for product signals (PFE2, PFE1) at $\delta = -82.0$ ppm has to be explained. Because this signal interferes with the signals of the starting material, the SE was determined by using the SNR of the hyperpolarized signal at $\delta = -82.0$ ppm, on the one hand, and the thermal SNR of the product CF_3 assumed from the separated thermal CF_2 signal at $\delta = -114.4$ or -117.8 ppm, on the other hand.

Analogous to the fluorine ALTADENA spectrum of PFE2 (Figure 4), the ^{19}F NMR spectrum of hyperpolarized PFE1 (Figure 5) was detected under the same hydrogenation conditions. For C-3″ ($\delta = -117.8$ ppm, SE = 10.5) and C-8″ ($\delta = -82.0$ ppm, SE = 18.8) two enhanced in-phase signals could be detected, whereas C-7″ ($\delta = -127.1$ ppm) shows an emission signal and C-4″ ($\delta = -124.5$ ppm) an anti-phase pattern, which were not enhanced.

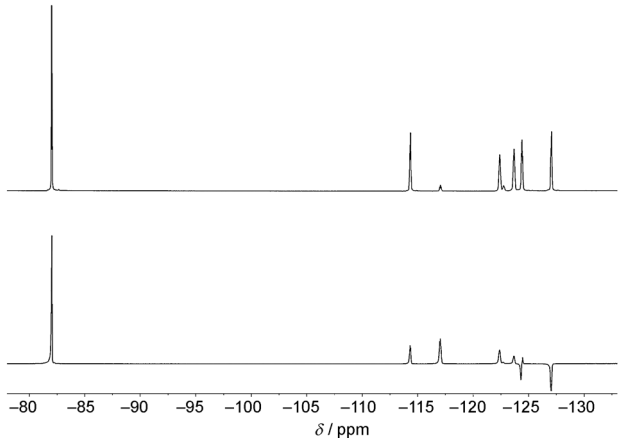

Figure 5. ^{19}F NMR spectrum taken directly after hydrogenation of PFE2 showing signals of hyperpolarized PFE1 (bottom) and the corresponding spectrum detected at thermal equilibrium (top).

Unexpectedly, in both cases a large portion of polarization is transferred to the CF_3 end groups, whereas the central moieties exhibited no signal improvement.

To clarify whether the relaxation times of the individual groups may explain this non-intuitive distribution of the polarization, T_1 values were measured by inversion recovery experiments for each fluorine group in PFE2 and PFE1 (Figure 6). The calculated longitudinal relaxation times range from 4.2 to 6.6 s, which renders it improbable that dif-

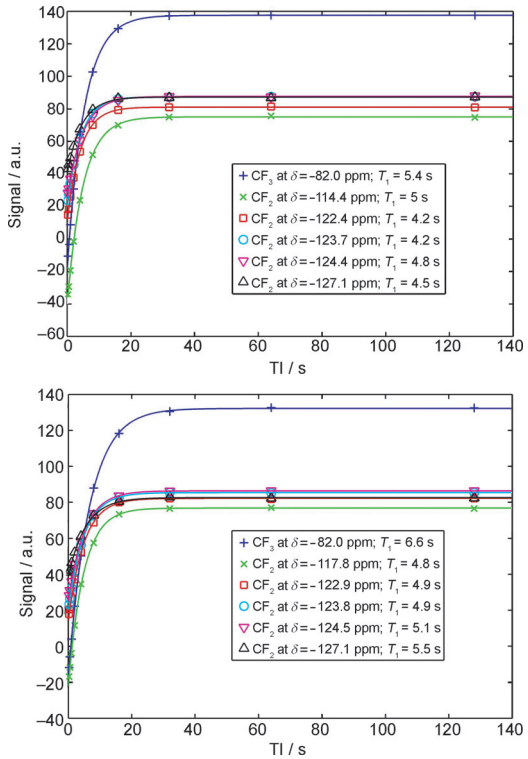

Figure 6. T_1 estimation from inversion recovery experiments. The fits for PFE2 (top) and PFE1 (bottom) yield relaxation times in the range of 4.2–6.6 s.

ferences in T_1 are the reason for the large variations in the SE factors obtained.

To obtain further information about the polarization transfer mechanism through the fluorinated alkyl chain and the differences in the observed signal enhancements between the middle and the exterior CF_2 or CF_3 groups, ^{19}F–^{19}F NOE measurements were performed. ^{19}F–^{19}F NOESY (nuclear Overhauser effect spectroscopy) provides unambiguous assignment of the vicinal fluorine atoms by showing through-space couplings.[18] Figure 7 shows the ^{19}F–^{19}F phase sensitive NOESY spectrum of PFE2 with a mixing time of 4 s (two scans, relaxation delay: 20 s).

In the ^{19}F–^{19}F NOESY spectrum of PFE2 in [D_6]acetone (Figure 7), two dominant pairs of cross peaks are observable for the signal of CF_3 (C-8′) at $\delta = -82.0$ ppm. These cross peaks reflect correlations to the lines at $\delta = -127.1$ and -123.6 ppm.

As known from ^{19}F–^{19}F COSY spectra, these signals correspond to CF_2 (C-7′, $\delta = -127.1$ ppm) and CF_2 (C 6′, $\delta = -123.6$ ppm) groups. This indicates interactions between closely related fluorine atoms. The third smaller NOESY connection corresponds to an interaction to the signal of CF_2 (C-5′, $\delta = -122.4$ ppm).

Similar results can be observed after closer examination of the cross peaks corresponding to the signal of C-3′ at $\delta = -114.4$ ppm. The strongest NOESY connections are assigned to the lines at $\delta = -124.4$ (C-4′) and -122.4 ppm (C-5′). Additionally, an interaction is observed for the cross peak at $\delta = -123.6$ ppm (C-6′).

There are remarkably strong in-phase cross peaks (same phase as diagonal peaks) at $\delta = -122.4/-124.4$ and $-124.4/-122.4$ ppm between the fluorine atoms on C-4′ and C-5′ in the middle of the fluorine alkyl chain as well as mixed phase signals at $\delta = -123.6/-124.4$ and $-124.4/-123.6$ ppm, respectively, which reveal a special connection between C-4′ and C-6′. No intensive cross peak can be measured for $\delta = -122.4/-123.6$ ppm (C-5′/C-6′).

The recorded ^{19}F–^{19}F NOESY spectrum of PFE1 shows a mixed-phase pattern between C-4“ and C-6” (see Figure S12 in the Supporting Information). In the spectrum of PFE3, the corresponding cross peaks (C-4 and C-6) could not be separated due to the absence of chemical shift differences.

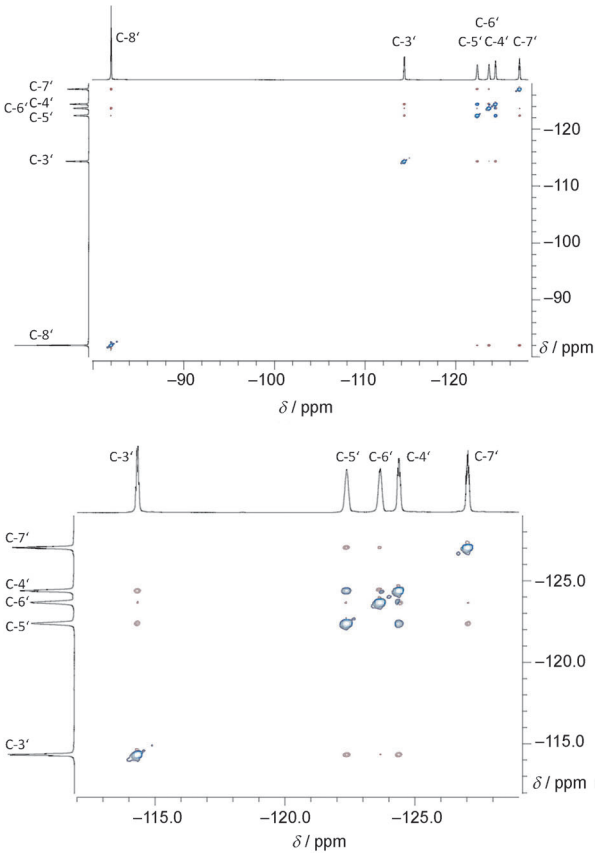

Figure 7. Full ^{19}F–^{19}F NOESY spectrum (282.5 MHz) of PFE2 in [D_6]acetone (top) and expansion of the ppm region between $\delta = -113.7$ and -128.0 ppm, where in-phase cross peaks (in comparison to the diagonal peaks) between C-4′ and C-5′ and mixed phase patterns between C-4′ and C-6′ are in evidence (bottom).

In contrast to PFE2, the correlations C-4/C-5 and C-4″/C-5″, respectively, are in opposite phase to the diagonal (spectra and values shown in the Supporting Information and Table 1).

So far, only Battiste et al. mentioned fluorine signals in ^{19}F–^{19}F NOESY spectra with a mixed-phase character for cyclic molecules.[19] Although signals with negative NOE (same phase as diagonal) were observed in different ^{19}F–^{19}F NOESY spectra shown in the literature, they were not interpreted.[17,20] These observations have not yet been

Table 1. Chemical shifts (δ), spin-lattice-relaxation times (T_1), signal enhancements (SE), observed couplings from ^{19}F–^{19}F COSY and NOESY spectra for PFE1 and PFE2 in degassed [D_6]acetone solution.

	PFE2						PFE1					
	C-3′	C-4′	C-5′	C-6′	C-7′	C-8′	C-3″	C-4″	C-5″	C-6″	C-7″	C-8″
δ [ppm]	−114.4	−124.4	−122.4	−123.7	−127.1	−82.0	−117.8	−124.5	−122.9	−123.8	−127.1	−82.0
T_1 [s]	5.0	4.8	4.2	4.2	4.5	5.4	4.8	5.1	4.9	4.9	5.5	6.6
SE	11	26	–	–	3	15	10.5	–	–	–	1.2	18.8
strong spin–spin coupling to	C-5′	C-6′	C-3′ C-7′	C-4′ C-8′	C-5′	C-6′	C-5″	C-6″	C-3″ C-7″	C-4″ C-8″	C-5″	C-6″
strong NOE to	C-4′ C-5′	C-3′ C-5′ C-6′	C-3′ C-4′ C-6′ C-7′	C-4′ C-5′ C-7′ C-8′	C-5′ C-6′ C-8′	C-6′ C-7′	C-4″ C-5″	C-3″ C-5″ C-6″	C-3″ C-4″ C-6″ C-7″	C-4″ C-5″ C-7″ C-8″	C-5″ C-6″ C-8″	C-6″ C-7″

clarified in detail. Strong coupling effects or cross-correlated dipole chemical shifts anisotropies are postulated as explanations for such phase changes.

To clarify whether the in-phase cross peaks in our case are based on this effects a 2D NOESY build-up curve was measured (Figure S14 in the Supporting Information). The results do not confirm an indirect NOE (no NOE build-up).

The opposite cross-peak phases of C4/C5 in the NOESY spectra of PFE2 and PFE1 do not explain the unexpected distribution of polarization in our PHIP data.

Therefore, intermolecular interactions were considered as an explanation of the polarization transfer to the end-standing CF_3 group. As those interactions (e.g., dipolar) should be a function of solvent polarity and/or substrate concentration, additional PHIP experiments with PFE3 in acetone and chloroform were performed by using varying concentrations. In Figure 8, the calculated SE factors for C-8′ and C-3′ are plotted. The diagrams clearly show a linear correlation between the SE factors of the two moieties, which does not change significantly for either solvents. Variations in the SE factors for certain concentrations result from the manual experimental procedure.

Hence, intermolecular polarization transfer could not be proven and the assumption and analysis of the intramolecular processes did not yield an explanation for the unexpected distribution of hyperpolarization. A complete theoretical analysis of these highly interesting systems is currently lacking. The read-out of all coupling constants from spectra, which can be measured at higher magnetic field, and numerical simulations should help to clarify the mechanism underlying the polarization distribution.

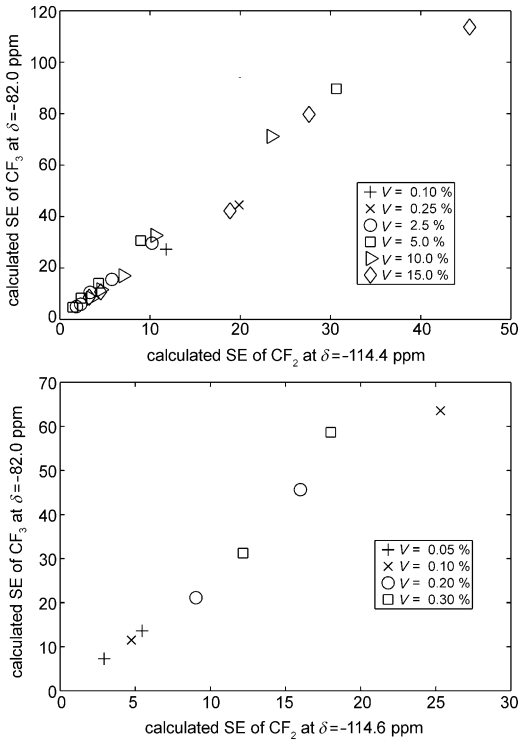

Figure 8. Calculated SE of the CF_2 group at $\delta = -114.6$ ppm plotted against the SE of the CF_3-group at $\delta = -82.0$ ppm for different concentrations (vol %) of PFE2 in [D_6]acetone (top) and [D_1]chloroform (bottom). As can be seen, all measurements show a stable ratio between the SEs for these groups.

This is the first time that PHIP has been used to generate ^{19}F hyperpolarization for an important biocompatible substrate. With regard to the use of clinically relevant perfluorocarbons, the observed polarization pattern qualifies the use of PFEs as interesting marker substances for MRI. Fortunately, the major part of the signal enhancement in PFE2 is located at $\delta = -82.0$ ppm, allowing the selection of the terminal CF_3 group for ^{19}F MRI. Figure 9 (left) shows an MR image of a phantom-containing hyperpolarized PFE2, which was acquired after hydrogenation of 0.075 mL PFE3 in acetone ($c = 0.071$ M).

The benefit of PHIP is clearly demonstrated by comparison with the image detected at thermal equilibrium (Figure 9, right).

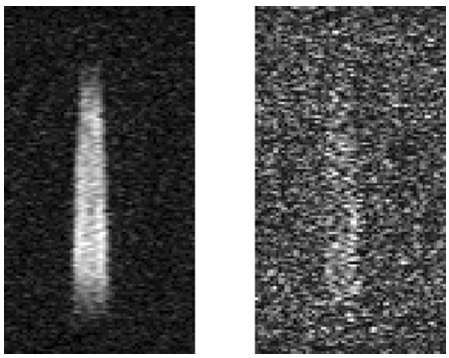

Figure 9. ^{19}F MR images of a PHIP experiment that uses a 0.071 M solution of PFE3 in [D_6]acetone. PFE2 after hyperpolarization (left) and in thermal equilibrium (right). Images were acquired at 4.7 T with a single scan by using a fast spin echo sequence (RARE: TE = 14 ms, FOV = 80 × 40, voxel size $0.625 \times 0.625 \times 1$ mm^3, RARE factor: 16, zero filling acceleration of two and acquisition time $t_{aq} = 465$ ms).

Conclusion

In summary, the analysis of the SE showed an unexpected degree of polarization transfer to the end-standing CF_3 group of the reaction products PFE2 and PFE1, respectively. Further investigation of this finding excluded intermolecular interactions as an explanation of this transfer of polarization over the rather long distance. However, the mechanism of the alternative intramolecular transfer could not yet be completely clarified. As the transfer only occurs in a low magnetic field, that is, in the strong coupling regime, the process seems to be driven by a *J*-coupling mechanism where the strong ^4J interactions may play a major role.

However, due to the strong SE and the notably well separated signal at $\delta = -82.0$ ppm, the end-standing CF_3 group is particularly well suited for ^{19}F imaging.

Future experiments at higher magnetic fields and corresponding simulations are necessary to elucidate the details of the polarization transfer along the fluorinated chain. A complete analysis of the relevant factors controlling this transfer will further improve the SE, thus enhancing the

SNR of corresponding MR spectra and images. The ^{19}F MR images of hyperpolarized PFE2 demonstrate that the spatial distribution of these biologically relevant semifluorinated alkenes should be detectable with mM concentration by using a single MR scan.

This qualifies the PHIP technique for a new class of potential biocompatible substances that do exhibit sufficient SE to allow background-free ^{19}F MRI as well as ^{19}F NMR spectroscopy.

Experimental Section

Materials: (Perfluoro-*n*-hexyl) acetylene (PFE3) and 1H,1H,2H-perfluoro-1-octene (PFE2) were purchased from ABCR, whereas (perfluoro-*n*-hexyl)ethane (PFE1) was delivered from Santa Cruz Biotechnology. The $[Rh^{I}(1,4\text{-bis(diphenylphosphino)-butane})\ (1,5\text{-cyclooctadiene})]BF_4$ catalyst was obtained from STREM Chemicals Inc. and the deuterated acetone from Deutero GmbH and euriso-top.

Hydrogenation and NMR measurements: Enriched para-H_2 (50%) was achieved at temperatures of liquid nitrogen over activated charcoal.[21] The samples consisted of PFE3/PFE2/PFE1 (0.2 mL), $[D_6]$acetone (1.8 mL), and the catalyst (0.014 mmol). Furthermore, the solutions were degassed under an argon atmosphere to remove oxygen. Then the parahydrogen (6.2 bar) was piped into a 10 mm NMR tube containing the prepared reaction solutions. The hydrogenations were performed under ALTADENA conditions by shaking the sample for about 10 s in the magnetic field of the earth. Then the tubes were transported into a 7 T Bruker WB 300 ultrashield NMR spectrometer. When the sample was locked (approximately 1–2 s after arriving at the lift-down position) data acquisition was started.

In the case of ^{1}H, a regular ALTADENA single-shot experiment with a 45° radio frequency pulse was performed (P1 = 14.5 μs, PL1 = 14.997 W). For ^{19}F PHIP experiments a 90° flip angle was used (P1 = 32.5 μs, PL1 = 17 W).

Signal enhancements: Signal enhancements specified in this work were calculated from the signal-to-noise ratios of the thermal and the hyperpolarized spectra by using Equation (1):

$$SE = \frac{\text{signal(HP)} \cdot \text{std(noise(thermal))}}{\text{std(noise(HP))} \cdot \text{signal(thermal)}} \quad (1)$$

Acknowledgements

This work was supported by the Deutsche Forschungsgemeinschaft (DFG BE 1824/8-1, BO 3055/2-1, BU 911/15-1. We thank the working group of Prof. Dr. Peter Spiteller, particularly Dipl.-Chem.-Ing. Johannes Stelten, for the opportunity to measure the proton-decoupled fluorine spectra.

[1] P. Kirsch, *Modern fluoroorganic chemistry*: Synthesis, reactivity, applications; Wiley-VCH, Weinheim, **2004**.
[2] C. Giraudeau, J. Flament, B. Marty, F. Boumezbeur, S. Mériaux, C. Robic, M. Port, N. Tsapis, E. Fattal, E. Giacomini, F. Lethimonnier, D. Le Bihan, J. Valette, *Magn. Reson. Med.* **2010**, *63*, 1119–1124.
[3] K. C. Lowe, *J. Mater. Chem.* **2006**, *16*, 4189.
[4] R. P. Mason, P. P. Antich, E. E. Babcock, J. L. Gerberich, R. L. Nunnally, *Magn. Reson. Imaging* **1989**, *7*, 475–485.
[5] a) S. Mizukami, R. Takikawa, F. Sugihara, Y. Hori, H. Tochio, M. Wälchli, M. Shirakawa, K. Kikuchi, *J. Am. Chem. Soc.* **2008**, *130*, 794–795; b) R. Schwarz, M. Schuurmans, J. Seelig, B. Künnecke, *Magn. Reson. Med.* **1999**, *41*, 80–86; c) G. Brix, M. E. Bellemann, H.-J. Zabel, P. Bachert, W. J. Lorenz, *Magn. Reson. Imaging* **1993**, *11*, 1193–1201; d) M. Plaumann, *Synthese und Charakterisierung paramagnetischer Kontrastmittel für die molekulare Bildgebung*, Shaker, Aachen, **2010**; e) A. Keliris, I. Mamedov, G. E. Hagberg, N. K. Logothetis, K. Scheffler, J. Engelmann, *Contrast Media Mol. Imaging* **2012**, *7*, 478–483.
[6] a) B. D. Ross, P. Bhattacharya, S. Wagner, T. Tran, N. Sailasuta, *AJNR Am J. Neuroradiol.* **2010**, *31*, 24–33; b) S. Aime, W. Dastrù, R. Gobetto, D. Santelia, A. Viale, *Handb. Exp. Pharmacol.* **2008**, *185*, 247–272; c) J. Leupold, S. Månsson, J. S. Petersson, J. Hennig, O. Wieben, *MAGMA* **2009**, *22*, 251–256; d) L. Schröder, T. J. Lowery, C. Hilty, D. E. Wemmer, A. Pines, *Science* **2006**, *314*, 446–449; e) K. Golman, J. H. Ardenkjaer-Larsen, J. S. Petersson, S. Mansson, I. Leunbach, *Proc. Natl. Acad. Sci. USA* **2003**, *100*, 10435–10439; f) E. J. R. van Beek, J. M. Wild, *Proc. Am. Thorac. Soc.* **2005**, *2*, 528.
[7] K. Golman, L. E. Olsson, O. Axelsson, S. Månsson, M. Karlsson, J. S. Petersson, *Br. J. Radiol.* **2003**, *76*, S118–S127.
[8] a) C. R. Bowers, D. P. Weitekamp, *Phys. Rev. Lett.* **1986**, *57*, 2645–2648; b) C. R. Bowers, D. P. Weitekamp, *J. Am. Chem. Soc.* **1987**, *109*, 5541–5542.
[9] a) M. G. Pravica, D. P. Weitekamp, *Chem. Phys. Lett.* **1988**, *145*, 255–258; b) J. Natterer, J. Bargon, *Prog. NMR Spectroscopy* **1997**, *31*, 293–315.
[10] a) M. Goldman, H. Jóhannesson, O. Axelsson, M. Karlsson, *Magn. Reson. Imaging* **2005**, *23*, 153–157; b) R. Rizi, P. Bhattacharya, E. Y. Chekmenev, W. F. Reynolds, S. Wagner, N. Zacharias, H. R. Chan, R. Bünger, B. D. Ross, *NMR Biomed.* **2011**, *24*, 925; c) D. Mayer, Y.-F. Yen, S. Josan, J. M. Park, A. Pfefferbaum, R. E. Hurd, D. M. Spielman, *NMR Biomed.* **2012**, *25*, 1119–1124.
[11] a) J. Barkemeyer, M. Haake, J. Bargon, *J. Am. Chem. Soc.* **1995**, *117*, 2927–2928; b) S. Bouguet-Bonnet, F. Reineri, D. Canet, *J. Chem. Phys.* **2009**, *130*, 234507; c) *Topics in Current Chemistry* (Eds.: J. Bargon, L. T. Kuhn), Springer, Berlin, **2007**; d) F. Reineri, A. Viale, G. Giovenzana, D. Santelia, W. Dastrù, R. Gobetto, S. Aime, *J. Am. Chem. Soc.* **2008**, *130*, 15047–15053; e) F. Reineri, A. Viale, S. Ellena, T. Boi, V. Daniele, R. Gobetto, S. Aime, *Angew. Chem.* **2011**, *123*, 7488–7491; *Angew. Chem. Int. Ed.* **2011**, *50*, 7350–7353; f) K. Golman, O. Axelsson, H. Jóhannesson, S. Månsson, C. Olofsson, J. S. Petersson, *Magn. Reson. Med.* **2001**, *46*, 1–5.
[12] U. Bommerich, T. Trantzschel, S. Mulla-Osman, G. Buntkowsky, J. Bargon, J. Bernarding, *PhysChemChemPhys* **2010**, *12*, 10309–10312.
[13] a) L. T. Kuhn, U. Bommerich, J. Bargon, *J. Phys. Chem. A* **2006**, *110*, 3521–3526; b) U. Bommerich, S. Mulla-Osman, J. Bargon, J. Bernarding, *Proc. Intl. Soc. Mag. Reson. Med.* **2009**, *17*, 2460.
[14] H. Meinert, T. Roy, *Eur. J. Ophthalmol.* **2000**, *10*, 189–197.
[15] Hendrik Hardung, PhD Thesis, Freiburg (Germany), **2008**.
[16] a) E. Wiberg, N. Wiberg, *Lehrbuch der anorganischen Chemie*, de Gruyter, Berlin, **1995**; b) N. S. Isaacs, *Physical Organic Chemistry*, Wiley, New York, **1995**.
[17] G. W. Buchanan, E. Munteanu, B. A. Dawson, D. Hodgson, *Magn. Reson. Chem.* **2005**, *43*, 528–534.
[18] J. L. Battiste, N. Jing, R. A. Newmark, *J. Fluorine Chem.* **2004**, *125*, 1331–1337.
[19] J. Battiste, R. A. Newmark, *Prog. NMR Spectroscopy* **2006**, 48, 1–23.
[20] S. Sato, J. Jida, K. Suzuki, M. Kawano, T. Ozeki, M. Fujita, *Science* **2006**, *313*, 1273–1276.
[21] K. F. Bonhoeffer, P. Harteck, *Z. Phys. Chem.* **1929**, *4*, 113–141.

Received: September 27, 2012
Revised: February 19, 2013
Published online: ■■ ■■, 0000

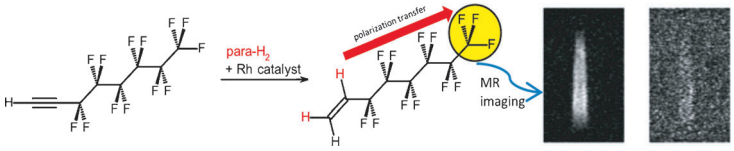

Fluorinated substances are important in chemistry and the life sciences. In a new approach, parahydrogen-induced polarization (PHIP) is applied to enhance ^{19}F MR signals of (perfluoro-*n*-hexyl)ethene and (perfluoro-*n*-hexyl)ethane. This allows ^{19}F MR imaging of hyperpolarized linear semifluorinated alkenes (see picture). Unexpectedly, the end-standing CF_3 group exhibits the highest amount of polarization despite the negligible coupling to the added protons.

Hyperpolarized Fluorine